J. Membrane Biol. 116, 129–137 (1990)

The Journal of
Membrane Biology

Characterization of Cl^- Transport in Vacuolar Membrane Vesicles Using a Cl^--Sensitive Fluorescent Probe: Reaction Kinetic Models for Voltage- and Concentration-Dependence of Cl^- Flux

Andrew J. Pope, Ian R. Jennings†, Dale Sanders†, and Roger A. Leigh
AFRC Institute of Arable Crops Research, Rothamsted Experimental Station, Harpenden, Hertfordshire AL5 2JQ, United Kingdom, and †Department of Biology, University of York, Heslington, York YO1 5DD, United Kingdom

Summary. The effects of Cl^- concentration and membrane potential ($\Delta\psi$) on Cl^- influx in isolated vesicles of vacuolar membrane (tonoplast) from red beet (*Beta vulgaris* L.) storage tissue have been characterized using the Cl^--sensitive fluorescent probe, 6-methoxy-1-(3-sulfonatopropyl)quinolinium (SPQ). The initial rate of Cl^- transport into the vesicles was enhanced both by the imposition of a positive $\Delta\psi$ and by increases in extravesicular Cl^- concentration. The kinetic mechanism underlying these responses was investigated by examining the accuracy with which the data could be described by several transport models. A model based on constant field theory yielded a poor description of the data, but satisfactory fits were generated by pseudo-two-state reaction kinetic models based on classical carrier schemes. Fits were equally good when it was assumed that charge translocation accompanied Cl^- entry, or when charge was carried by the unloaded transport system, as long as only a single charge is translocated in each carrier cycle. Expansion of the models to three states enabled description of the Cl^- concentration dependence of transport by changes in a single, voltage insensitive rate constant which is tentatively identified with Cl^- binding at the external surface of the membrane. The derived value of the dissociation constant between Cl^- and the transport system is estimated at between 30 and 52 mM.

Key Words *Beta* · Cl^--transport · 6-methoxy-1-(3-sulfonatopropyl)quinolinium · membrane potential · reaction kinetic model · vacuolar membrane vesicles

Introduction

The accumulation of Cl^- within the vacuole of higher plants is important both for the generation of turgor and the homeostasis of cytoplasmic Cl^- concentration (Flowers, 1988). In giant algae, such as *Chara* or *Nitella*, the electrochemical potential gradient for Cl^- requires active transport of this ion from the cytoplasm to the vacuole (MacRobbie, 1970). This may involve a H^+/Cl^- antiport but, as yet, there is only a small amount of evidence to support the presence of H^+-coupled anion transport systems in the vacuolar membrane, the tonoplast (*see* Schumaker & Sze, 1987). However, there is evidence for a Cl^- uniport that allows transport of Cl^- into the vacuole in response to the inside positive membrane potential ($\Delta\psi$) generated by the tonoplast ATP- and pyrophosphate-dependent H^+-pumps (Bennett & Spanswick, 1983; Kaestner & Sze, 1987; Pope & Leigh, 1987). Nevertheless, detailed studies of the relationship between $\Delta\psi$ and Cl^- influx have not been made.

Recently, we described the use of a Cl^--sensitive fluorescent probe, 6-methoxy-1-(3-sulfonatopropyl)quinolinium (SPQ), to measure Cl^- transport in isolated tonoplast vesicles (Pope & Leigh, 1988). This probe can be used to report quantitatively, and in real time, changes in the Cl^- concentration within vesicles (Illsley & Verkman, 1987; Pope & Leigh, 1988). In work published elsewhere (Pope & Leigh, 1990), we have demonstrated that this technique can be used to measure electrically driven Cl^- influx in the presence of K^+-diffusion potentials generated using K^+ concentration gradients and valinomycin. Now we report a detailed study of the effects of artificially imposed $\Delta\psi$'s on the initial rate of Cl^- transport in tonoplast vesicles from red beet storage tissue. The kinetic mechanism underlying these responses has been investigated by least-squares fitting of a variety of transport models to the data.

Materials and Methods

Red beet (*Beta vulgaris* L. cv. Detroit Crimson Globe) was grown in a glasshouse and storage roots were harvested immediately before use. The Cl^--sensitive dye, 6-methoxy-1-(3-sulfonatopropyl)quinolinium (SPQ), was synthesized and purified as described previously (Wolfbeis & Urbano, 1982; Pope & Leigh,

1988). Other chemicals were purchased from either Sigma or B.D.H. Chemicals (both of Poole, Dorset, UK).

Tonoplast vesicles were prepared using the modification of the method of Rea and Poole (1985) described previously (Pope & Leigh, 1988). Vesicles were loaded with SPQ and K^+ by incubation for 30 min at 37°C in a medium containing 20 mM SPQ, 0.485 M sorbitol, 5 mM K_2SO_4, 10 mM N-[2-hydroxy-1,1-*bis*(hydroxymethyl)ethyl]glycine (tricine)-1,3,-*bis*[tris(hydroxymethyl)methylamino]propane (BTP), pH 7.4, 1 mM dithiothreitol (DTT) and 1 mM ethylenediaminetetraacetic acid (EDTA)-BTP, pH 7.4. They were then washed three times in ice-cold SPQ-free medium (340,000 × *g*; Beckman Type 70.1 Ti rotor) to remove extravesicular probe. Loaded vesicles were used either immediately or were stored at −70°C. Freezing did not affect either SPQ loading or rates of Cl^- transport.

Measurements of SPQ fluorescence were made at 25°C in a stirred cell, using a Perkin-Elmer LS5 fluorimeter (Perkin-Elmer Instruments, Beaconsfield, Bucks, UK). The excitation wavelength was 350 nm and emission was measured using a total fluorescence attachment and a 420-nm glass cut-off filter, to maximize the signal obtained. Assays (2 ml volume) were performed in a medium containing 10 mM tricine-BTP, pH 7.4, 5 μM valinomycin, and sufficient sorbitol to maintain iso-osmolarity with the vesicles (Pope & Leigh, 1988). To impose K^+-diffusion potentials, the concentration of K_2SO_4 in the assay medium was varied and the resultant potential was calculated from the Nernst equation. Varying the external or internal concentration of K_2SO_4 had no direct effect on either Cl^- transport or the response of SPQ (Pope & Leigh, 1990).

Transport was initiated by adding an aliquot of vesicles to the assay medium. The time course of SPQ fluorescence was then recorded on an IBM PC-XT microcomputer using the software described by Jennings et al. (1988). A falling exponential was fitted to the data and the initial rate of change of intravesicular Cl^- concentration ($d[Cl]_i/dt$ for $t = 0$) was then calculated from the known response of SPQ fluorescence to Cl^- concentration, as described previously (Pope & Leigh, 1988; *see also* Illsley & Verkman, 1987). Curve fitting was performed using the nonlinear least-squares algorithm of Marquardt (1963). The initial rate of change of intravesicular Cl^- concentration is directly proportional to true Cl^- flux and so the two terms are used interchangeably.

The magnitudes of the imposed K^+ diffusion potentials (and hence the membrane potential, $\Delta\psi$) were not confirmed experimentally. However, previous work has shown that the intravesicular K^+ concentration can be specified by the incubation procedure used to load SPQ and K^+ into the vesicles (Pope & Leigh, 1990). The experimental procedure used to measure transport ensured that diffusion potentials were imposed only when the vesicles were added to the assay medium. Transport is reported as the initial Cl^- influx and, at this time, the potential should be that specified by the Nernst equation on the reasonable assumption that, in the presence of valinomycin, the permeability of the vesicles to K^+ will be very much greater than that to Cl^- or SO_4^{2-}. At later times, net KCl transport will have occurred and the size of the potential is not known with certainty.

To compensate for variation in absolute Cl^- flux between vesicle preparations, the results of each experiment were weighted in the following way. First, each value in an individual data set was expressed relative to the mean of the values obtained between −10 and +10 mV for that set. The resultant relative data were then converted back to absolute units of Cl^- flux by multiplying each value by the absolute mean flux observed between −10 and +10 mV for *all* data sets at a given Cl^- concentration. Using the mean of the values between −10 and +10 mV avoided errors associated with weighting all of the data to a single datum point at 0 mV.

Results and Discussion

Figure 1 shows typical fluorescence traces from an experiment to determine the effect of K^+-diffusion potentials on Cl^- influx in tonoplast vesicles from red beet. The imposition of positive K^+-diffusion potentials increased both the initial rate and the extent of SPQ quenching, indicating electrically driven Cl^- uptake. This was observed at all Cl^- concentrations tested (*see also* Pope & Leigh, 1990). More detailed experiments tested the effects of membrane potentials in the range −30 to +70 mV, at external Cl^- concentrations between 5 and 50 mM. Each set of conditions was replicated two or three times with different vesicle preparations. These experiments resulted in the generation of a family of flux-voltage (*F-V*) curves that describe the response of Cl^- influx to $\Delta\psi$ at different external Cl^- concentrations (Fig. 2).

Examination of the *F-V* curves reveals a number of features. First, positive potentials increased Cl^- influx at all external Cl^- concentrations. Second, negative potentials, imposed using $[K^+]_{out}/[K^+]_{in}$ ratios of less than one, reduced influx relative to that observed at 0 mV. Third, at external Cl^- concentrations of 10 mM or less, the response to $\Delta\psi$ was sigmoidal, as found in other experiments (Pope & Leigh, 1990). However, as the Cl^- concentration was increased, this feature became less pronounced, and the response to $\Delta\psi$ became more linear (Fig. 2). To gain information about the possible kinetic mechanisms underlying the responses of Cl^- influx to $\Delta\psi$ and Cl^- concentration, several transport models were fitted to the data.

On the assumption that influx was through a simple channel, we attempted to describe the data with a conventional model based on constant field theory (Goldman, 1943). Here, the unidirectional flux (J_{Cl}), which in these experiments is identical to the net flux because the initial intravesicular Cl^- concentration was zero, is described by the Ussing-Teorell relationship:

$$J_{Cl} = \frac{P_{Cl} \cdot F \cdot [Cl]_s \cdot \Delta\psi}{RT\left[1 - \exp\frac{-F \cdot \Delta\psi}{RT}\right]} \quad (1)$$

where P_{Cl} is the Cl^- permeability of the membranes, $[Cl]_s$ is the extravesicular Cl^- concentration, and R, T and F have their usual meanings. In this scheme only one parameter, P_{Cl}, is unknown. The modeling strategy is therefore to constrain the value of $[Cl]_s$ for each of the curves to the known Cl^- concentra-

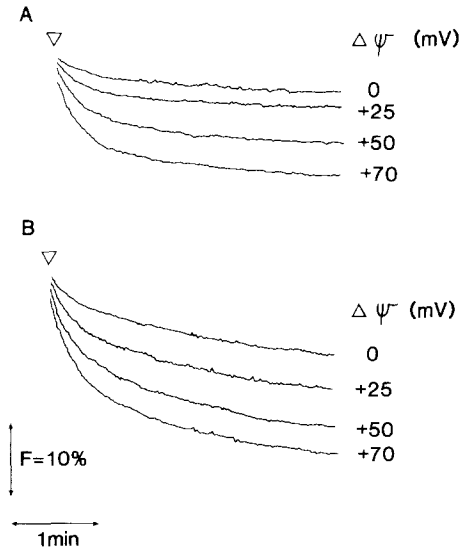

Fig. 1. Effect of K^+-diffusion potentials on the time course of quenching of the fluorescence of SPQ in tonoplast vesicles from red beet in the presence of an inwardly directed Cl^- concentration gradient of 10 (*A*), or 50 (*B*) mM. Vesicles, loaded with SPQ, 10 mM tricine-BTP, pH 7.4, 0.485 M sorbitol and 5 mM K_2SO_4, were added at (▽) to iso-osmotic media containing either (*A*) 10 or (*B*) 50 mM Cl-BTP, pH 7.4, 10 mM tricine-BTP, pH 7.4, 5 μM valinomycin, sorbitol, and sufficient K_2SO_4 to give the indicated membrane potential

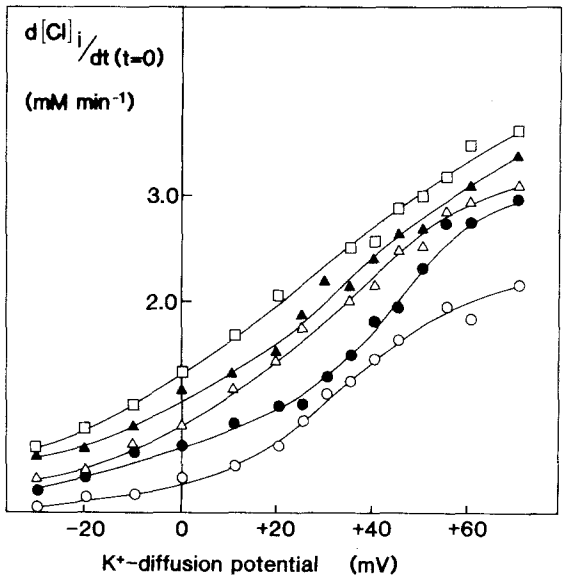

Fig. 2. Effect of K^+-diffussion potentials on the initial rate of Cl^- transport into tonoplast vesicles from red beet, in the presence of inwardly directed Cl^- concentration gradients of 5 (○), 10 (●), 20 (△), 30 (▲), or 50 (□) mM Cl^-. Experimental conditions were as described in the legend in Fig. 1. Results are the mean of two or three experiments and have been weighted by the method described in the text. Lines were fitted by eye

tion and to try to find a common value of P_{Cl} which describes all of the curves. Figure 3 shows the best fit which can be obtained in this way. It is clear that this simple model cannot describe the data.

The model fails because it predicts that, at any given $\Delta\psi$, flux is a linear function of $[Cl]_s$. Figure 4 shows clearly, for four sample transmembrane potentials, that Cl^- flux is a saturable function of $[Cl]_s$, as found in previous experiments (Pope & Leigh, 1987, 1988). Moreover, the concentration dependence of the flux can be described, at any given $\Delta\psi$, by a single Michaelis-Menten function. As $\Delta\psi$ became more positive, J_{max} increased and K_m decreased. The quantitiative implications of this finding are discussed below. For present purposes, however, it is sufficient to note that the kinetic behavior of transport with respect to concentration implies (*i*) that a single transport system is being studied and (*ii*) that the data might be more accurately described by models which embody saturation kinetics.

Reaction-state kinetic carrier models have previously been successfully applied to describe the current-voltage (*I-V*) relationships of a number of primary pumps (Sanders, Hansen & Slayman, 1981; Gradmann, Hansen & Slayman, 1982; Slayman & Sanders, 1985) and secondary transport systems (Sanders & Hansen, 1981; Sanders et al., 1984;

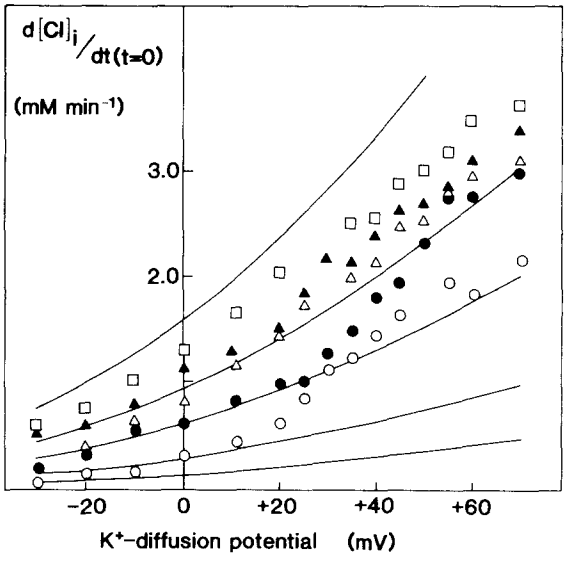

Fig. 3. Best fits obtained when attempts were made to describe the data shown in Fig. 2 using a simple "channel" model based on constant field theory. Symbols indicate measured Cl^- influx at 5 (○), 10 (●), 20 (△), 30 (▲), or 50 (□) mM $[Cl]_s$. Solid lines show predicted rates from the best fit of the data to the Ussing-Teorrel relationship (Eq. (1)). Fitting yielded a value of P_{Cl} of 32.2 min^{-1}

Sanders, 1986; Blatt, Rodriguez-Navarro & Slayman, 1987; Sanders, Hopgood & Jennings, 1989) as well as ion channels (Gradmann, Klieber & Hansen, 1987; Bertl, Klieber & Gradmann, 1988; Bertl

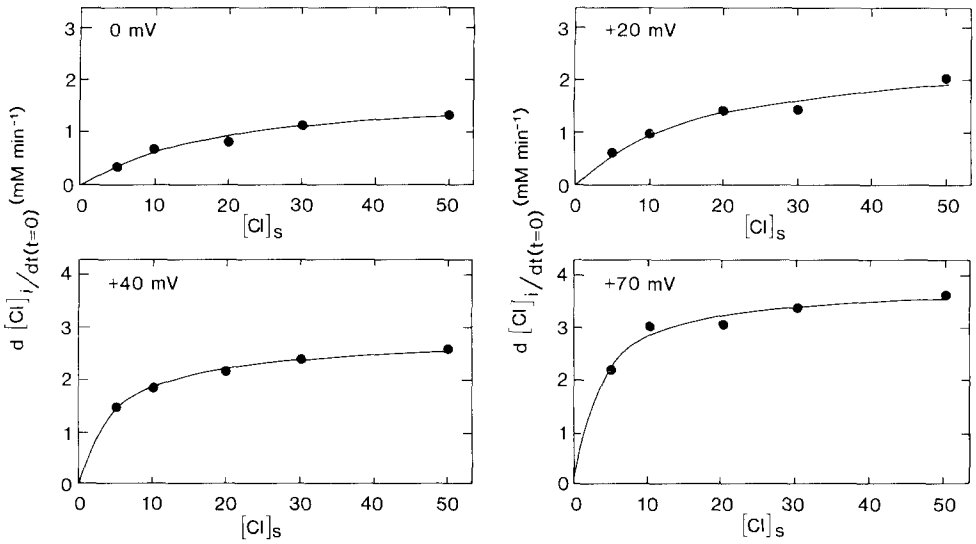

Fig. 4. Relationships between Cl^- influx and Cl^- concentration at membrane potentials of 0, +20, +40 and +70 mV. Data from Fig. 2 replotted and fitted by Michaelis-Menten relationships. Derived Michaelis-Menten parameters are as follows:

$\Delta\psi$ (mV)	J_{max} (mM · min^{-1})	K_m (mM)
0	1.92 ± 0.20	22.1 ± 4.9
+20	2.59 ± 0.27	16.8 ± 4.4
+40	2.75 ± 0.07	4.8 ± 0.6
+70	3.80 ± 0.13	3.6 ± 0.6

1989; *see* Sanders, 1990, for a review). It seemed that such models might prove useful for modeling the *F-V* data.

Our strategy for fitting carrier models to the present data was to begin by consideration of a two-state model (*see* inset, Fig. 5). It has been shown previously (Hansen et al., 1981) that any given *I-V* relationship for an electrogenic transport system containing just one charge translocation step can be described by this simple model. A corollary of this finding is that higher order models cannot be used for curve-fitting to single *I-V* (or *F-V*) relationships because the number of degrees of freedom exceeds the information implicit in the data; a unique model cannot, therefore, be derived.

The two-state model explicitly retains the electrogenic step (denoted by the inward and outward rate constants k_{21} and k_{12}, respectively), but lumps all electroneutral reactions into two gross rate constants [denoted as K_{21} (inward) and K_{12} (outward)]. Voltage dependence in the charge translocating reaction is introduced as a symmetric Eyring barrier (Lauger & Stark, 1970):

$$k_{21} = k_{21}^0 \exp\left[\frac{-z \cdot F \cdot \Delta\psi}{2RT}\right]$$

$$\text{and } k_{12} = k_{12}^0 \exp\left[\frac{z \cdot F \cdot \Delta\psi}{2RT}\right] \quad (2,\text{ab})$$

where k^0 indicates the value of the specified rate constant at 0 mV, and z is the stoichiometry of charge (with appropriate polarity) translocated per carrier cycle.

Although it is, in principle, possible to determine the four two-state rate constants from a single data set, considerably greater confidence in the parameter estimates results from joint fitting of several *F-V* data sets at different ligand concentrations. Joint fitting involves optimizing the estimate for a given parameter, but constraining that estimate to a common value for all data sets. The relevant relationship between current (or net flux) and the reaction constants of the two-state model has been derived by Hansen et al. (1981) and is given as:

$$J_{Cl} = z \cdot N\left[\frac{K_{21} \cdot k_{12} - K_{12} \cdot k_{21}}{k_{12} + k_{21} + K_{12} + K_{21}}\right] \quad (3)$$

where J_{Cl} is the net Cl^- flux and N is the overall carrier density (which serves merely as a scaling factor, and in all curve fitting is constrained to unity). It is important to note that for an anionic transport system, z is positive if the carrier-ion complex is electrically neutral and charge is translocated on the unloaded carrier, or negative if the unloaded carrier is neutral and charge translocation

accompanies that of the ion. In the zero-*trans* conditions of the present experiments, where efflux of Cl^- is not possible, K_{12} must be constrained to zero in the former case, whereas in the latter case, this experimental condition results in $K_{21} = 0$. [The rationale for this simplification becomes apparent when a lumped K reaction constant is expressed in terms of "real" rate constants (Sanders, 1988). The resultant expression comprises a numerator which is simply the product of all "real" unidirectional rate constants facing in the same direction as the lumped rate constant, and any associated ligand concentrations. Since intravesicular Cl^- is absent, the entire K reaction constant becomes zero; *see* Eq. (8), *below*.]

Figure 5 shows the results of joint fitting the ensemble of data in Fig. 2 to Eq. (3) for the case of an electrically neutral unloaded carrier with charge translocation accompanying that of Cl^- (i.e., $z = -1$). The result is a reasonable description of the data. The fit is equally good if the effect of $[Cl]_s$ on the *F-V* relationship is via k^0_{12} *or* k^0_{21}, with the alternate voltage-sensitive rate constant and K_{12} held common for all data sets. If, by contrast, the effect of $[Cl]_s$ is allowed to reside in K_{12} with the two voltage-sensitive rate constants constrained, poor fits result (*data not shown*). Correspondingly good fits were obtained for complementary case of a neutral carrier-ion complex (i.e., $z = +1$; *data not shown*). Again, adequate fits were obtained only if the effect of $[Cl]_s$ was exerted via either of the voltage-sensitive rate constants. Cases in which z was constrained to integer values other than ± 1 failed to yield adequate fits (*data not shown*).

At first sight, it appears paradoxical that $[Cl]_s$ should exert its effect on the voltage-sensitive rate constants. However, there is a theoretical basis for this effect which arises from reduction of the "real" multi-state model to a two-state model (Hansen et al., 1981). The process of model reduction in effect violates the Law of Conservation of Mass by embedding in the two carrier states all "hidden" states. A consequence of this is that the hidden rate constants of the real multi-state model become embedded in all four two-state rate constants. However, expansion of the two-state model, if performed in conjunction with group fitting of the series of *F-V* curves, can be used to identify explicit reaction constants and therefore correctly localize the ligand binding reaction. Thus a three-state model is employed for further fitting.

The inset to Fig. 6 shows the three-state model for an electrically neutral unloaded carrier. The gross voltage-insensitive reaction constants are now subdivided into two separate limbs which make explicit the Cl^- binding and dissociation reactions on both sides of the membrane. The Cl^- flux for the three-state model is given as:

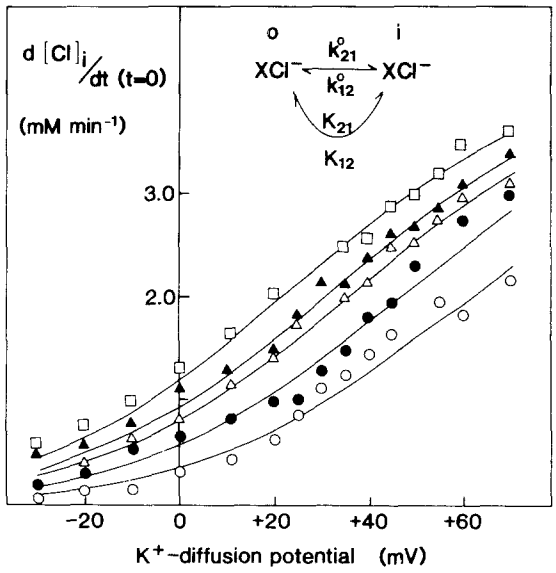

Fig. 5. Best fits obtained to the data shown in Fig. 2 using a two-state reaction kinetic model, assuming an electrically neutral unloaded carrier. The inset shows a schematic representation of the reaction scheme. Symbols indicate measured rates of Cl^- influx at 5 (○), 10 (●), 20 (△), 30 (▲), or 50 (□) mM $[Cl]_s$. For this fit, only the rate constant k^0_{21} was allowed to vary between curves. Fitting yielded the following values for the various rate constants (±SE):

Rate constant		sec^{-1}
k^0_{12}		0.197 ± 0.059
K_{12}		0.075 ± 0.004
K_{21}		0.00
k^0_{21}	5 mM Cl^-	0.028 ± 0.006
	10 mM Cl^-	0.045 ± 0.010
	20 mM Cl^-	0.064 ± 0.016
	30 mM Cl^-	0.074 ± 0.019
	50 mM Cl^-	0.103 ± 0.029

$$J_{Cl} = z \cdot N \left[\frac{k_{12} \cdot K_{23} \cdot K_{31} - k_{21} \cdot K_{32} \cdot K_{13}}{k_{12}(K_{23} + K_{32} + K_{31}) + K_{13}(k_{21} + K_{32} + K_{23}) + k_{21}(K_{31} + K_{32}) + K_{31} \cdot K_{23}} \right] \quad (4)$$

where k_{21} and k_{12} retain their functions of describing inward and outward charge translocation, respectively. Again, for the zero-*trans* conditions, and in the case of an electrically neutral unloaded carrier, K_{31} has been constrained to zero for all fitting.

The results of fitting the three-state model are shown in Fig. 6*A*. The case presented (that for variation of K_{32} with Cl^- concentration, with all other parameters held to constant optimized values for the five data sets) represents the best fit that could be obtained with the three-state model. It is therefore satisfying that the effects of Cl^- concentration

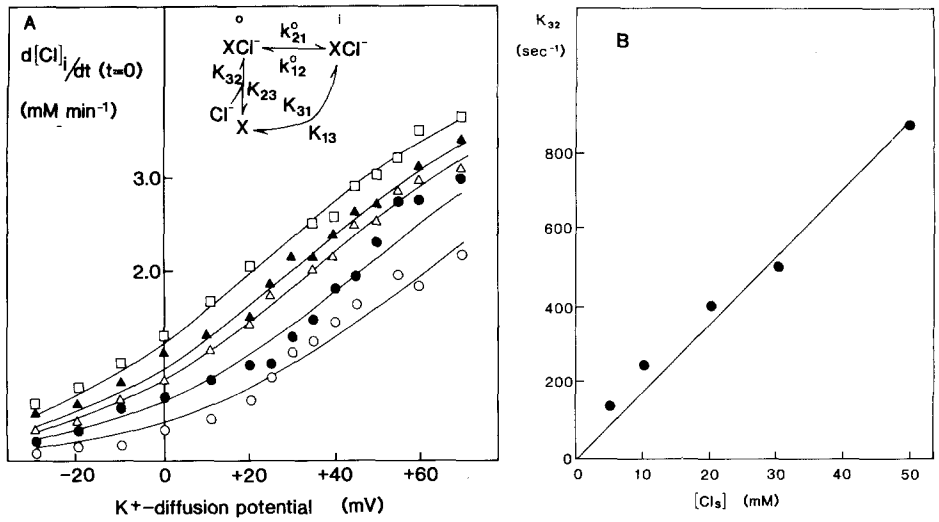

Fig. 6. (*A*) Best fit obtained to the data shown in Fig. 2 using a three-state reaction kinetic model, assuming an electrically neutral unloaded carrier. Inset shows a schematic diagram of the reaction cycle. Symbols indicate measured Cl^- influx at 5 (○), 10 (●), 20 (△), 30 (▲), or 50 (□) mM $[Cl]_s$. Lines indicate predicted rates from fits obtained when only K_{32} was allowed to vary between curves. Fitting yielded the following values for the rate constants (±SE):

Rate constant		sec^{-1}
k^0_{12}		0.197
k^0_{21}		0.212
K_{23}		9.26×10^2
K_{31}		0.00
K_{13}		0.075
K_{32}	5 mM Cl^-	141.5 ± 6.12
	10 mM Cl^-	247.8 ± 10.5
	20 mM Cl^-	402.0 ± 18.3
	30 mM Cl^-	510.0 ± 24.9
	50 mM Cl^-	874.2 ± 53.5

(*B*) Dependence of the value of K_{32} on $[Cl]_s$. The line indicates a least-squares fit to the data, with the intercept constrained to zero. The slope of the line is 17.9 ± 0.8 $mM^{-1} \cdot sec^{-1}$ which yields a value for $K^0_{32} = 1.79 \times 10^4\ M^{-1} \cdot sec^{-1}$

can now be isolated at the single rate constant that would, *a priori* be expected to be that involving binding of extravesicular Cl^-. Relative values for the five rate constants optimized by fitting are given in the figure legend. The corresponding fit for the case of a neutral carrier-ion complex, where the effect of $[Cl]_s$ is allowed to reside with K_{23}, and K_{13} is constrained to zero (*not shown*) was equally good.

An independent check on the validity of the three-state model parameters can be performed by comparing them with the rate constants derived from the two-state fits. Gradmann et al. (1987) have shown that the two-state parameters can be described in terms of their three-state counterparts by the following relationships:

$$k^0_{12}\ (\text{2-state}) = \frac{k^0_{12}(K_{32} + K_{31})}{K_{32} + K_{31} + K_{13}}\ (\text{3-state}) \tag{5}$$

$$k^0_{21}\ (\text{2-state}) = \frac{k^0_{21}(K_{32} + K_{31})}{K_{32} + K_{31} + K_{23}}\ (\text{3-state}) \tag{6}$$

$$K_{12}\ (\text{2-state}) = \frac{K_{32} \cdot K_{13}}{K_{32} + K_{31} + K_{13}}\ (\text{3-state}) \tag{7}$$

$$K_{21}\ (\text{2-state}) = \frac{K_{23} \cdot K_{31}}{K_{32} + K_{31} + K_{23}}\ (\text{3-state}). \tag{8}$$

Substituting the values in the legend to Fig. 6 into the right-hand sides of Eqs. (5) to (8) yields estimates of the two-state parameters at $[Cl]_s$ = 5 mM of $k^0_{12} = 0.197\ sec^{-1}$, $k^0_{21} = 0.0281\ sec^{-1}$, $K_{12} = 0.075\ sec^{-1}$ and $K_{21} = 0$, respectively. Refer-

ence to Fig. 5 (legend) shows that these estimates are in excellent accord with those derived independently for the two-state model, and similarly good agreement is apparent at the other values of $[Cl]_s$.

The reasons why variation of $[Cl]_s$ can be localized kinetically solely to the voltage-sensitive k_{21}^0 rate constant of the two-state model are now clear. Although the three-state rate constant, K_{32}, which putatively subsumes Cl^- binding, appears in all four two-state reaction constants, its presence in Eqs. (5) and (7) is hidden because it constitutes the dominant term in both the numerators and the denominators ($K_{32} \gg K_{13}$, and $K_{31} = 0$). In the case of the other nonzero two-state reaction constant (k_{21}^0, Eq. (6)), the much larger value of K_{23} prevents domination of the denominator by K_{32}. Nevertheless, as K_{32} rises with $[Cl]_s$, the two-state parameter k_{21}^0 should tend to saturation because the disparity between K_{23} and K_{32} decreases. Saturation of k_{21}^0 with increasing $[Cl]_s$ is apparent (Fig. 5, legend). However K_{32} does not saturate with $[Cl]_s$.

If indeed K_{32} does subsume Cl^- binding, it can be expanded as:

$$K_{32} = K_{32}^0 \cdot [Cl]_s \tag{9}$$

where K_{32}^0 is the value of the constant at 1 M $[Cl]_s$. Figure 6*B* demonstrates that K_{32} displays a linear dependence on $[Cl]_s$ in accord with Eq. (9), despite the fact that this relationship was not assumed as part of the curve-fitting procedure. The ratio K_{23}/K_{32}^0 defines the dissociation constant for Cl^-, resulting in a value (*see* legend to Fig. 6) of 51.8 mM.

We have already noted that activation of Cl^- transport by increasingly positive $\Delta\psi$ occurs kinetically both through an increase in J_{max} and a decrease in K_m for transport (Fig. 4, legend). Are the features of the three-state model competent to replicate this finding quantitatively? The answer is yes. The three-state relationship describing flux as a function of the six rate constants (Eq. (4)) can, after substituting $K_{31} = 0$, be recast in Michaelis-Menten formalism as:

$$J_{Cl} = \frac{J_{max} \cdot [Cl]_s}{K_m + [Cl]_s} \tag{10}$$

where

$$J_{max} = \frac{N \cdot k_{21} \cdot K_{13}}{k_{12} + K_{13} + k_{21}} \tag{11}$$

and

$$K_m = \frac{k_{12} \cdot K_{23} + K_{13} \cdot K_{23} + k_{21} \cdot K_{13}}{K_{32}^0(k_{12} + K_{13} + k_{21})}. \tag{12}$$

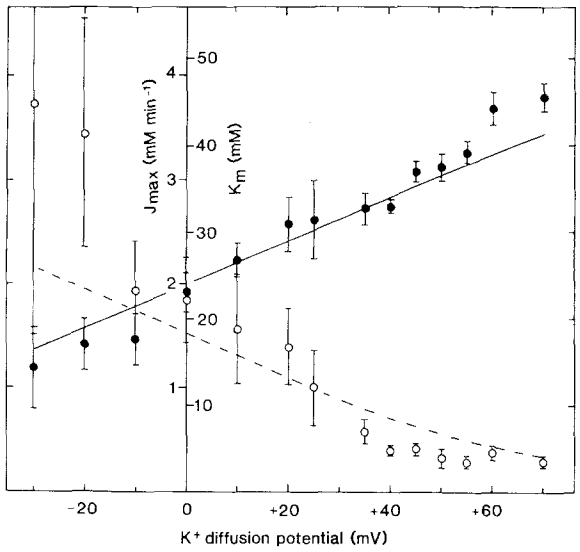

Fig. 7. Response of J_{max} (●——●) and K_m (○——○) to $\Delta\psi$. Data points are derived from least-squares fitting of single Michaelis-Menten relationships to the data of Fig. 2. Lines show the responses of J_{max} and K_m to $\Delta\psi$ based on the rate constants of the three-state model (Fig. 6, legend) and Eqs. (11) and (12). A value of K_{32}^0 (2.83×10^4 $M^{-1} \cdot sec^{-1}$) based on the three-state model estimate of K_{32} at 5 mM Cl^- (141.5 sec^{-1}) is used for numerical evaluation of Eq. (12), since flux at 5 mM Cl^- has a disproportionate effect on the least-squares estimate of K_m

Estimates of J_{max} and K_m were obtained at each $\Delta\psi$ by nonlinear least-squares fitting, as in Fig. 4, and the results are shown in Fig. 7. The dependence of J_{max} on $\Delta\psi$ predicted by the three-state parameters (Fig. 6 legend, and Eq. (11)) provides an excellent description of the observed response of J_{max} over the $\Delta\psi$ range −30 to +70 mV; the predicted increase in J_{max} is 2.5-fold over this voltage range, while the observed increase is 3.2-fold. The direct least-squares estimates of K_m rely heavily on the accuracy of the flux measurement at the lowest $[Cl]_s$ (= 5 mM; *see* Fig. 4), and a value of K_{32}^0 derived from the estimate of K_{32}^0 at 5 mM Cl^- has therefore been substituted into Eq. (12) along with the other parameters from the three-state model. Again, the result is a reasonable predicted dependence of the Michaelis parameter on $\Delta\psi$, though experimental uncertainties on the actual value of K_m for low fluxes (i.e., at negative $\Delta\psi$) preclude detailed assessment over the whole range of $\Delta\psi$. The higher value of K_{32}^0 used for description of the $\Delta\psi$-dependence of K_m compared with the mean value of K_{32}^0 derived from the data of Fig. 6 (2.83×10^4 compared with 1.79×10^4 M^{-1} sec^{-1}) results in a lower estimate of the dissociation constant for Cl^- binding (30.2 mM in Fig. 7, compared with 51.8 mM in Fig. 6).

The results of this study are in accord with previous analyses based on single-channel studies (Gradmann et al., 1987) and macroscopic behavior of ion channels in plants (Fisahn, Hansen & Gradmann, 1986) in demonstrating the utility of classical, carrier-type models in describing kinetic properties of channels in plant membranes. We conclude that the Cl^- uniporter at the tonoplast of red beet exhibits saturable binding of the ion and that Cl^- binds with a voltage-independent dissociation constant in the region of 30–50 mM. However, the data do not allow us to distinguish whether charge translocation accompanies movement of the ion or that of the unloaded carrier.

The present analysis is restricted to consideration of channel properties at the macroscopic level. The opening frequency of individual channels is assumed to be invariant with membrane potential, i.e., the possibility that the channels are voltage gated is not explicitly considered. However, in view of the excellent description of the macroscopic flux-voltage relationships afforded by the reaction kinetic analysis, there is clearly no justification at present for extension of the models to incorporate the contingency of voltage gating. Thus, our data suggest that an adequate description of the kinetic behavior of the Cl^- channel need not invoke voltage-dependent opening, though whether such voltage gating actually occurs will be most accurately addressed in future work by investigations at the single-channel level (Bertl & Gradmann, 1987; Laver & Walker, 1987; Bertl et al., 1988; Sanders, 1990).

Financial support to I.R.J. and D.S. from the Agricultural and Food Research Council (Grant AG87/29) is gratefully acknowledged. We are also deeply indebted to Professor C.L. Slayman (Yale University) for providing us with the "joint fitting" routines which made the reaction kinetic analysis possible.

References

Bennett, A.B., Spanswick, R.M. 1983. Optical measurements of ΔpH and $\Delta\psi$ in corn root membrane vesicles: Kinetic analysis of Cl^- effects on a proton-translocating ATPase. *J. Membrane Biol.* **71**:95–107

Bertl, A. 1989. Current-voltage relationships of a sodium-sensitive potassium channel in the tonoplast of *Chara corallina*. *J. Membrane Biol.* **109**:9–19

Bertl, A., Gradmann, D. 1987. Current-voltage relationships of potassium channels in the plasmalemma of *Acetabularia*. *J. Membrane Biol.* **99**:41–49

Bertl, A., Klieber, H.-G., Gradmann, D. 1988. Slow kinetics of a potassium channel in *Acetabularia*. *J. Membrane Biol.* **102**:141–152

Blatt, M.R., Rodriguez-Navarro, A., Slayman, C.L. 1987. Potassium-proton cotransport in *Neurospora:* Kinetic control by pH and membrane potential. *J. Membrane Biol.* **98**:169–189

Fisahn, J., Hansen, U.-P., Gradmann, D. 1986. Determination of charge, stoichiometry and reaction constants from *I-V* curve studies on a K^+ transporter in *Nitella*. *J. Membrane Biol.* **94**:245–252

Flowers, T.J. 1988. Chloride as a nutrient and an osmoticum. *In:* Advances in Plant Nutrition. P.B. Tinker and A. Läuchli, editors. Vol. 3, pp. 55–78. Praeger, New York

Goldman, D.E. 1943. Potential, impedance and rectification in membranes. *J. Gen. Physiol.* **27**:37–60

Gradmann, D., Hansen, U.-P., Slayman, C.L. 1982. Reaction-kinetic analysis of current-voltage relationships for electrogenic pumps in *Neurospora* and *Acetabularia*. *Curr. Top. Membr. Transp.* **16**:257–276

Gradmann, D., Klieber, H.-G., Hansen, U.-P. 1987. Reaction kinetic parameters for ion transport from steady-state current-voltage curves. *Biophys. J.* **51**:569–585

Hansen, U.-P., Gradmann, D., Sanders, D., Slayman, C.L. 1981. Interpretation of current-voltage relationships for "active" ion transport systems: I. Steady-state reaction-kinetic analysis of class-I mechanisms. *J. Membrane Biol.* **63**:165–190

Illsley, N.P., Verkman, A.S. 1987. Membrane chloride transport measured using a chloride-sensitive fluorescent probe. *Biochemistry* **26**:1215–1219

Jennings, I.R., Rea, P.A., Leigh, R.A., Sanders, D. 1988. Quantitative and rapid estimation of H^+ fluxes in membrane vesicles. Software for analysis of fluorescence quenching and relaxation. *Plant Physiol.* **83**:483–489

Kaestner, K.H., Sze, H. 1987. Potential-dependent anion transport in tonoplast vesicles from oat roots. *Plant Physiol.* **83**:483–489

Lauger, P., Stark, G. 1970. Kinetics of carrier-mediated ion transport across lipid bilayer membranes. *Biochim. Biophys. Acta* **552**:458–466

Laver, D.R., Walker, N.A. 1987. Steady-state voltage-dependent gating and conduction kinetics of single K^+ channels in the membrane of cytoplasmic drops of *Chara australis*. *J. Membrane Biol.* **100**:31–42

MacRobbie, E.A.C. 1970. The active transport of ions in plant cells. *Q. Rev. Biophys.* **3**:251–294

Marquardt, D.W. 1963. An algorithm for least squares estimation of non-linear parameters. *J. Soc. Ind. Appl. Math.* **11**:431–441

Pope, A.J., Leigh, R.A. 1987. Some characteristics of anion transport at the tonoplast of oat roots, determined from the effects of anions on pyrophosphate-dependent proton transport. *Planta* **172**:91–100

Pope, A.J., Leigh, R.A. 1988. The use of a chloride-sensitive fluorescent probe to measure chloride transport in isolated tonoplast vesicles. *Planta* **176**:451–460

Pope, A.J., Leigh, R.A. 1990. Characterisation of chloride transport at the tonoplast of higher plants using a chloride-sensitive fluorescent probe. Effects of membrane potential, other ions, and transport inhibitors on chloride flux. *Planta* (*in press*)

Rea, P.A., Poole, R.J. 1985. Proton-translocating inorganic pyrophosphatase of red beet (*Beta vulgaris* L.) tonoplast vesicles. *Plant Physiol.* **77**:46–52

Sanders, D. 1986. Generalized kinetic analysis of ion-driven cotransport systems: II. Random ligand binding as a simple explanation of non-Michaelian kinetics. *J. Membrane Biol.* **90**:67–87

Sanders, D. 1988. Steady-state kinetic analysis of chemiosmotic proton circuits in microorganisms. *In:* Physiological Models

in Microbiology. M.J. Bazin and J.I. Prosser, editors. Vol. I, pp. 49–74. CRC, Boca Raton (FL)

Sanders, D. 1990. Kinetic modeling of plant and fungal membrane transport systems. *Annu. Rev. Plant Physiol. (in press)*

Sanders, D., Hansen, U.-P. 1981. Mechanism of Cl^- transport at the plasma membrane of *Chara corallina:* II. Transinhibition and the determination of H^+/Cl^- binding order from a reaction kinetic model. *J. Membrane Biol.* **58:**139–153

Sanders, D., Hansen, U.-P., Gradmann, D., Slayman, C.L. 1984. Generalized kinetic analysis of ion-driven cotransport systems: A unified interpretation of selective ionic effects on Michaelis parameters. *J. Membrane Biol.* **77:**123–152

Sanders, D., Hansen, U.-P., Slayman, C.L. 1981. Role of the plasma membrane proton pump in pH regulation in non-animal cells. *Proc. Natl. Acad. Sci. USA* **78:**5903–5907

Sanders, D., Hopgood, M., Jennings, I.R. 1989. Kinetic response of H^+-coupled transport to extracellular pH: Critical role of cytosolic pH as a regulator. *J. Membrane Biol.* **108:**253–261

Schumaker, K.H., Sze, H. 1987. Decrease of pH gradients in tonoplast vesicles by NO_3^- and Cl^-: Evidence for H^+-coupled anion transport. *Plant Physiol.* **83:**490–496

Slayman, C.L., Sanders, D. 1985. Steady-state kinetic analysis of an electroenzyme. *Biochem. Soc. Symp.* **50:**11–29

Wolfbeis, O.S., Urbano, E. 1982. Synthesis of fluorescent dyes. XIV. Standards for fluorescence measurements in the near-neutral pH range. *J. Heterocyc. Chem.* **19:**841–843

Received 7 September 1989; revised 17 January 1990